Magnetic Susceptibility Anisotropy of Central Nervous System

C. Liu[1,2]
[1]Brain Imaging and Analysis Center, Duke University, Durham, NC, United States, [2]Radiology, Duke University, Durham, NC, United States

INTRODUCTION:

Magnetic susceptibility difference between brain gray and white matter results in strong phase contrast between these two types of tissues at high magnetic field strength (*1, 2*). Here, we report, for the first time, a surprising observation of tissue-level magnetic susceptibility anisotropy in the central nervous system (CNS) using a mouse model. Specifically, we propose a method for calculating intrinsic susceptibility maps by solving three complementary equations. This method removes a common streaking artifact. More importantly, we found that susceptibility of the white matter exhibits strong orientation dependence. Such orientation variation is extensive throughout the white matter area, but is relatively weak in the gray matter. We anticipate that imaging this anisotropy will provide a unique tissue contrast that is unknown previously. In addition, it will provide a novel tool to further quantify the substructures of the central nervous system.

METHODS:

High-resolution MRI experiments were conducted on a fixed mouse brain. The study was approved by our Institutional Animal Care and Use Committee. The brain was kept in the cranium to avoid damages to the brain caused by surgical removal. The specimen was sealed tightly inside a cylindrical tube. To allow free rotation, the tube was contained within and taped to a hollow sphere. The sphere containing the specimen was placed inside a dual-channel mouse coil. 3D spoiled-gradient-recalled-echo (SPGR) images were acquired using a 7.0T horizontal bore magnet at an isotropic spatial resolution of 85.9 μm. The echo time (TE) was 8 ms and sequence repetition time was 100 ms. After each acquisition, the sphere was rotated to a different orientation and the acquisition was repeated.

A 3D frequency map was calculated for each orientation. Prior to the calculation of the frequency map, raw phase images were high-pass filtered to remove a slowly varying global phase similar to methods described by previous authors (*2-4*). To determine the intrinsic value of magnetic susceptibility and to reduce a common streaking artifacts existing in the numerically computed susceptibility maps, we propose to solve three equations simultaneously using the LSQR algorithm. The first equation is described through a Fourier transform (FT) relationship (*5, 6*) as shown in Eq. [1]; the second equation is generated by taking a first-order partial differentiation of the first equation with respect to spatial frequency coordinates; the third equation in the image-domain is provided by the basic laws for magnetic induction expressed by the Green function. Although Eq. [1] provides an accurate solution for majority locations in the frequency domain, there is also a region where the coefficients are zero thus prohibiting the inversion. Together, the three equations proposed here complement each other and eliminate the possibility of null coefficients existing in Eq. [1].

$$\theta(\mathbf{r}) = FT^{-1}\left\{\left(\frac{1}{3}-\frac{k_z^2}{k^2}\right)\chi(\mathbf{k})\right\}\gamma H_0 t \qquad [1]$$

$$2k_z\theta(\mathbf{k}) + k^2\theta'_{k_z}(\mathbf{k}) = \gamma H_0 t\left(-\frac{4}{3}k_z\chi(\mathbf{k}) + \left(\frac{1}{3}k^2 - k_z^2\right)\chi'_{k_z}(\mathbf{k})\right) \qquad [2]$$

$$\theta(\mathbf{r}) = \gamma H_0 t\left(g_y(\mathbf{r}) * \chi'_y(\mathbf{r}) + g_x(\mathbf{r}) * \chi'_x(\mathbf{r}) - \frac{2}{3}\chi(\mathbf{r})\right) \qquad [3]$$

RESULTS:

Figure 1a shows examples of frequency maps acquired at different orientations. Although the frequency maps clearly indicate orientation dependence, this variation is a result of both a spatially distributed susceptibility and a geometric factor. Thus it is not a definitive evidence of bulk susceptibility anisotropy. Figure 1b shows susceptibility maps computed for the same four orientations as shown in Figure 1a. Anisotropic susceptibility is clearly evident in the white matter as shown in Figure 1b. White matter tissue can appear bright or dark depending on their relative orientation with respect to the main field. Figure 1c plots the susceptibility value as a function of the orientation for two representative voxels: one in the gray matter and one in the white matter. The anisotropy is relatively weak in the gray matter as shown by the voxel comparison in Figure 1c.

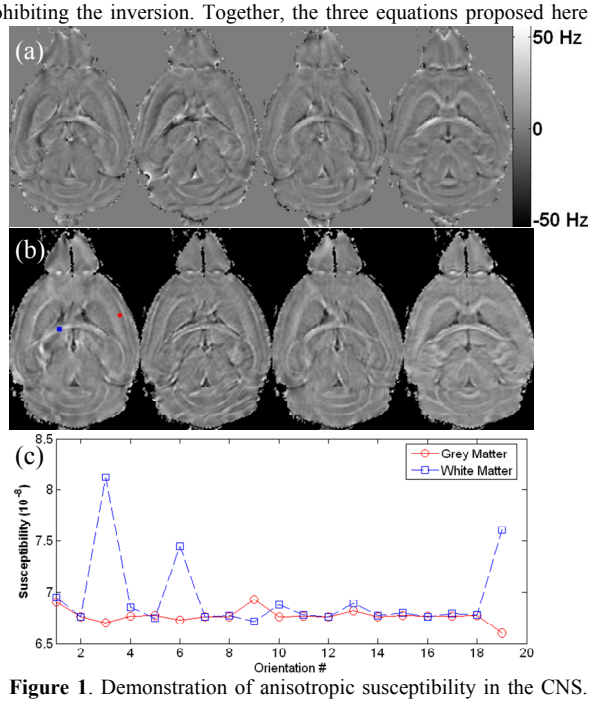

Figure 1. Demonstration of anisotropic susceptibility in the CNS. (a) Maps of frequency offset measured at four representative orientations illustrating orientation dependence. (b) Intrinsic susceptibility maps at the same four orientations clearly demonstrating the existence of susceptibility anisotropy. (c) Plot of susceptibility values of two voxels as a function of orientation. Gray matter shows relatively weak anisotropy while white matter shows strong anisotropy.

DISCUSSIONS AND CONCLUSIONS:

Our study shows that susceptibility anisotropy exists for water confined in the space of white matter. Although it has been known that some molecules exhibit anisotropic susceptibility, it is surprising that bulk susceptibility anisotropy can be observed in water protons of the brain. Even in complex heterogeneous environments, the NMR spectrum of water protons usually consists of a single resonance peak. In 3D MR images of the central nervous system (CNS), billions of macromolecules exist in one imaging voxel and their interaction with each other is complex and intractable. However, the particular structure of axons seems to force a common symmetry among the molecules such that they are aligned to a certain degree. This alignment results in a spatial network of macroscopically observable magnetic susceptibility anisotropy in the white matter of CNS.

Our results open new avenues for generating image tissue contrast in the CNS based on magnetic susceptibility anisotropy. This anisotropy can be intrinsic tissue property; it can also be induced by the introduction of exogenous molecular agents.

ACKNOWLEDGMENTS:

The study is supported by the National Institutes of Health (NIH) through grant R00EB007182.

REFERENCES:

1. A. Rauscher, J. Sedlacik, M. Barth, H. J. Mentzel, J. R. Reichenbach, *AJNR Am J Neuroradiol* **26**, 736 (Apr, 2005).
2. J. H. Duyn *et al.*, *Proc Natl Acad Sci U S A* **104**, 11796 (Jul 10, 2007).
3. E. M. Haacke, Y. Xu, Y. C. Cheng, J. R. Reichenbach, *Magn Reson Med* **52**, 612 (Sep, 2004).
4. A. Rauscher *et al.*, *Magn Reson Imaging* **26**, 1145 (Oct, 2008).
5. L. Li, *Magn Reson Med* **46**, 907 (Nov, 2001).
6. D. S. B. Salomir R, Moonen CTW, , *Concepts in Magnetic Resonance Part B* **19B**, 26 (2003).